



# OPEN Gibbsian surface thermodynamic analysis of emulsion liquid membranes

Shaghayegh Sadeghi & Leila Zargarzadeh✉

The emulsion liquid membrane is a promising technique for separating pollutants such as metals, weak acids and bases, mineral species, hydrocarbons, and biological substances. The popularity of the membrane process is due to its high mass transfer efficiency, process simplicity, and low energy consumption. Despite significant advancements in the field of emulsion liquid membranes, the effect of the interfacial curvature on component distribution remains largely uninvestigated. In the present study, considering the emulsion liquid membrane where no reaction takes place, the thermodynamic equilibrium relationships are calculated while considering the effect of interfacial curvature between the phases. The Gibbsian surface thermodynamic method is employed to derive the equations at equilibrium for the composite system of emulsion liquid membrane. With the obtained equations, the mole fraction and percentage extraction of the desired substance can be calculated under various conditions, such as different surfactant concentration, and droplet size, as well as assuming ideal or non-ideal condition for the solution. The results indicate that by reducing the size of internal droplets to the nanoscale, the effect of interfacial curvature becomes significant, and the extraction percentage gets higher.

**Keywords** Emulsion liquid membrane, Double emulsion, Gibbsian composite-system thermodynamics, Interfacial curvature, Multiphase multicomponent system

Around half a century ago, Li made a significant discovery regarding emulsion liquid membranes (ELMs), revealing their substantial potential as efficient tools for a diverse range of separation processes<sup>1</sup>. ELMs are typically created by combining two immiscible phases to form an emulsion, which is then dispersed in a third continuous phase through agitation, for extraction<sup>2</sup>. The liquid phase that separates the internal droplets from the external continuous phase is known as the membrane phase<sup>2</sup>. The membrane phase allows specific components to pass through it selectively, moving from the external phase to the internal droplets and vice versa<sup>2</sup>. The emulsion may have one of the two following forms: oil/water/oil (O/W/O), as shown in Fig. 1, or water/oil/ water (W/O/W), with the water or oil as the membrane phase, respectively<sup>2</sup>. The combination of internal phase droplets inside a droplet of a membrane phase is called a globule.

There are two types of separation mechanisms: simple and facilitated<sup>2</sup>. A simple permeation mechanism happens due to difference in chemical potential of the specific component between the internal and external phases, and reasonable solubility and diffusivity of that component in the membrane<sup>2</sup>. On the other hand, there are two types of facilitated mechanisms: In type I, the mass transfer is increased by using a stripping agent in the receiving phase (internal phase when the feed is the external phase, and vice versa). Then the target diffusing species reacts with the chemical stripping agent in the receiving phase, which creates a product that cannot diffuse back through the membrane, and the separation happens<sup>2</sup>. The second type is called carrier-facilitated transport, where a carrier compound transports the diffusing species, and reactions occur at the two interfaces of external-membrane and internal-membrane<sup>2</sup>.

In general, the process of ELM, preparation, and extraction, consists of four steps<sup>3</sup>, as presented in Fig. 2:

1. The membrane and internal phases are emulsified.
2. The emulsion gets dispersed in the continuous phase.
3. The emulsion and external phases settle after extraction.
4. De-emulsification is carried out to recover the membrane phase.

Faculty of Chemical Engineering, Amirkabir University of Technology (Tehran Polytechnic), Tehran, Iran. ✉email: zargarzadeh@aut.ac.ir

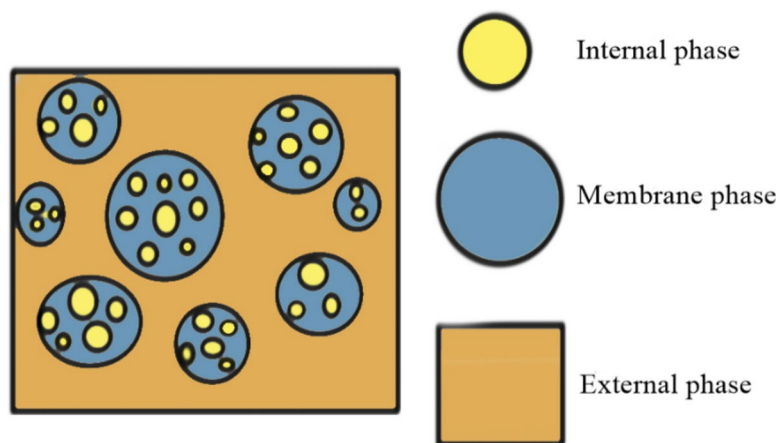


**Fig. 1.** Schematic of the ELM, oil-in water-in oil (O/W/O) type, the internal and external phases are oil and the membrane phase is water.

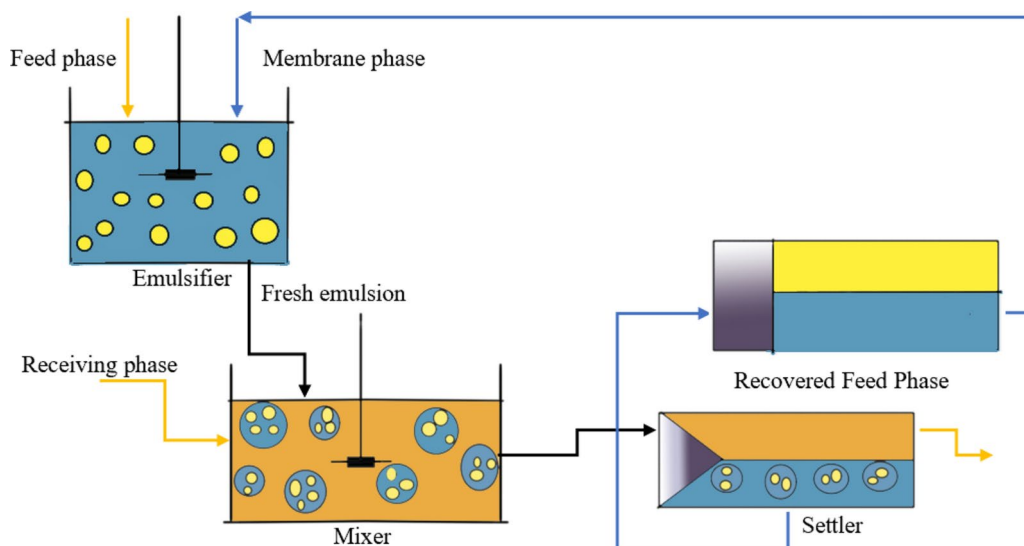


**Fig. 2.** Flow diagram of the batch mixer-settler operation for emulsion liquid membrane (ELM).

Since the discovery of ELMs, there have been many studies and experiments exploring emulsion liquid membrane, its general functioning<sup>2</sup>, and ways to enhance stability<sup>4–10</sup> by adjusting factors like impeller speed, carrier, surfactants, pH, and temperature as the instability of the emulsion globules against fluid shear and osmotic swelling has been a challenge for many scientists. Emulsion liquid membranes have been applied in various areas, including removing metals like gold and copper<sup>3,7,11,12</sup>, treating wastewater<sup>13–15</sup>, extracting phenol and other organic pollutants<sup>8,13,14,16–18</sup>, and separating hydrocarbons<sup>1,10,19</sup> for which the small differences in boiling points have made other separation methods to be challenging. Emulsion liquid membranes have also proven useful in recovering biomolecules and other biological products<sup>20–23</sup>. There are also recent works incorporating ionic liquids into ELMs (called EILM) in removal of components from aqueous solutions such as removal of lead<sup>24</sup>, cationic dye<sup>25</sup>, or lactic acid<sup>26</sup>. Despite the significant progress made in the field of emulsion liquid membranes, there remain opportunities for further research and development. There is limited existing research on the thermodynamic stability of emulsion liquid membranes<sup>27–29</sup>. However, the effect of fluid interface curvature on the component distribution after reaching the (pseudo) equilibrium remains unexplored. To address this gap, here we investigate the distribution of components between the internal and the external phases in O/W/O ELM with no reaction, using Gibbsian composite-system thermodynamics. It should be noted that while emulsions are inherently non-equilibrium systems, the system in this study is kinetically at equilibrium, as with the use of surfactant and low surface tension, the process of droplets merging toward stable equilibrium occurs slowly. Therefore, the ELM can be considered to be in pseudo-equilibrium. This treatment has been successfully applied in previous studies, considering several bubbles and a local supersaturation, by Ward and Levart<sup>30</sup>, and Zargarzadeh and Elliott<sup>31</sup>. Our investigation of a non-reactive ELM system reveals the component distribution between the phases, influenced by the pressure difference of the phases.

## System definition and governing equations

The chosen system is from an experimental study with the purpose of separating toluene from n-heptane<sup>10</sup>, which are not easily separated by conventional distillation as their boiling points are close. The initial feed is therefore a mixture of toluene and n-heptane that makes the internal droplets. The membrane phase is mainly water with dissolved sodium lauryl sulfate as an emulsifying agent, and the external phase is initially made of n-dodecane<sup>10</sup>. The separation of toluene from n-heptane is based on the selectivity which arises from distinct permeation rates of each component through the membrane phase<sup>1</sup>. Also, there is a selective solubility of toluene in the water, compared to negligible solubility of n-heptane and n-dodecane, only toluene can transfer through the membrane phase, from the higher chemical potential to the lower one until the system evolves to the equilibrium. The solubility of toluene, n-heptane and n-dodecane in water at 298.15 K and 1 atm are 0.52, 0.003, and in the range of  $3.7 \times 10^{-7}$  to  $8.42 \times 10^{-7}$  gr component/gr water, respectively<sup>32–34</sup>. In the absence of a membrane, n-dodecane and n-heptane are also miscible, and the system is in a single-phase state. However, due to the presence of a selective permeable membrane, only toluene permeates from the internal phase towards the membrane phase<sup>1</sup>. Eventually, toluene diffuses from the membrane phase into the external phase containing n-dodecane, and it dissolves. However, n-heptane remains in the internal phase, and n-dodecane remains in the external phase.

The initial mass fractions of toluene and n-heptane in the feed are 0.5<sup>10</sup>. According to the chosen experimental study<sup>10</sup>, 1 ml of the internal phase in membrane emulsion is dispersed in 3 ml of the external phase at 298.15 Kelvin<sup>10</sup>. The concentration of sodium lauryl sulfate (SLS) in the aqueous (membrane) phase of the experimental study<sup>10</sup> is lower than 1% (w/v). Consequently, in our modeling, we considered the concentration of SLS in the membrane phase to be negligible to avoid the complexities associated with activity coefficient interaction parameters. It is important to note that we accounted for the effect of adding surfactant by considering a range of values for interfacial tension (presented in section "The effect of the interfacial tension, due to the surfactant"). Further improvement can be made by using a model that express surface tension as a function of surfactant concentration, provided that parameters for such models are available. The size of internal droplets is considered to be constant, representing the average diameter of the internal droplets. The breakage and swelling of the emulsion are neglected. Summary of all the assumed and experimental variable values are presented in Table 1.

The thermodynamic analysis involves considering a composite system of ELMs in terms of its constituent simple subsystems. A simple system is one in which the intensive properties of the system remain constant at equilibrium<sup>35</sup>. The subsystems within the emulsion liquid membrane system consist of three different phases: internal, membrane, and external, along with two interfaces between the membrane-internal and membrane-external phases. One globule (a number of internal droplets inside one membrane droplet), and the encompassing external phase is considered as the system of interest, as shown in Fig. 3.

When reaching equilibrium condition, the external phase has n-dodecane and the transferred toluene, the membrane phase has water and some toluene, and the internal droplets consist of n-heptane and the remaining toluene. A significant amount of toluene has migrated from the internal phase to the external phase.

According to the Gibbsian thermodynamics for multiphase systems, equilibrium conditions are obtained from the fact that the entropy of an isolated composite system (system and its reservoir) at equilibrium reaches an extremum amount, or in other words, the derivative of the entropy of the system and its reservoir is zero<sup>35</sup>.

$$dS^{res} + dS^L + dS^{LM} + dS^M + dS^{MD} + dS^D = 0 \quad (1)$$

$d$  and  $S$  are the differential term and entropy. Superscripts  $res$ ,  $L$ ,  $M$ ,  $D$ ,  $LM$ ,  $MD$  are used for the reservoir, external phase, membrane phase, internal droplet phase, interface of external-membrane and interface of internal-membrane, respectively.

Category	Variable	Value/Description
Initial Conditions Assigned variables from the experiments <sup>10</sup>	Phases and components before equilibrium	Internal: Toluene, n-heptane Membrane: Water, surfactant(negligible) External: n-dodecane
	Initial mass fractions of toluene + n-heptane mixture	Toluene: 0.5, n-heptane: 0.5
	$f$ : ratio of the external phase to the emulsion phase	$f = 3$ 1 mL of emulsion dispersed in 3 mL of external phase
	Temperature	298.15 K
	Pressure	1 atm
	Surfactant (SLS) in the membrane phase	Negligible compared to water
Assumptions	Internal droplet radius, membrane radius	Set the values, representing the average diameter
	$B$ : packing fraction of the membrane globule by the droplets (equivalent to setting number of droplets in the membrane)	0.83
	Emulsion breakage and swelling	Neglected
	Liquid membrane permeability	Selective, allowing only toluene to pass through

**Table 1.** Summary of the assigned variables and assumptions for the emulsion liquid membrane system.

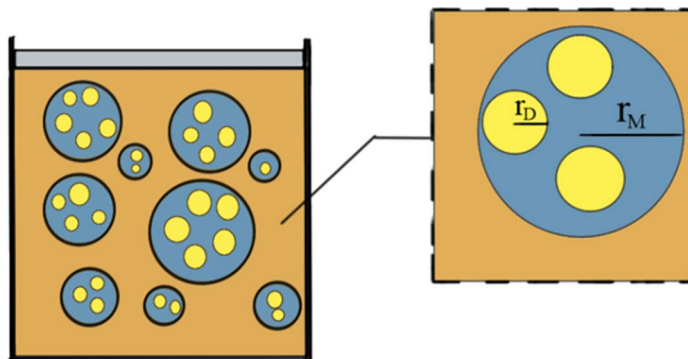


**Fig. 3.** Schematic of the O/W/O ELM system and the considered system., which is one globule (several internal droplets inside one membrane droplet), and the encompassing external phase.  $r_D$  and  $r_M$  are radius of internal droplet and globule, respectively. The size of internal droplets is considered constant, equal to the average diameter.

For the reservoir and each of the three bulk phases, the differential form of the fundamental equation of thermodynamics is:

$$dS^\alpha = \frac{1}{T^\alpha} dU^\alpha + \frac{P^\alpha}{T^\alpha} dV^\alpha - \sum_{i=1}^m \frac{\mu_i^\alpha}{T^\alpha} dn_i^\alpha \quad (2)$$

where  $S^\alpha$ ,  $T^\alpha$ ,  $U^\alpha$ ,  $P^\alpha$ ,  $V^\alpha$  are the entropy, temperature, internal energy, pressure, and volume, respectively, for phase  $\alpha$  (such as *res*, *L*, *M*, or *D*). Also,  $\mu_i^\alpha$  and  $n_i^\alpha$  are the chemical potential and number of moles of component  $i$  in phase  $\alpha$ , and  $m$  is the number of components in the bulk phase.

The Gibbsian surface of tension approximation is used for the curved interfaces, placing the dividing interface in such a way that the interfacial tension becomes independent of the curvature. In this case, all components will be present at the common interface. For the entropy of curved interfaces therefore, the following relationship holds:

$$dS^{\alpha\beta} = \frac{1}{T^{\alpha\beta}} dU^{\alpha\beta} - \frac{\sigma^{\alpha\beta}}{T^{\alpha\beta}} dA^{\alpha\beta} - \sum_{i=1}^k \frac{\mu_i^{\alpha\beta}}{T^{\alpha\beta}} dn_i^{\alpha\beta} \quad (3)$$

where  $S^{\alpha\beta}$ ,  $T^{\alpha\beta}$ ,  $U^{\alpha\beta}$ ,  $\sigma^{\alpha\beta}$ ,  $A^{\alpha\beta}$ ,  $\mu_i^{\alpha\beta}$  and  $n_i^{\alpha\beta}$  represent entropy, temperature, internal energy, interfacial tension, area, chemical potential of component  $i$ , and number of moles of component  $i$  at the  $\alpha\beta$  interface, and  $k$  stands for the number of components present at that interface. Using the Gibbs surface of tension approximation approach<sup>35</sup>, the interfacial tension is not explicitly dependent on the curvature or the size of the droplet. Rather, its dependence is implicit, manifesting through variations in the intensive state parameters<sup>36,37</sup>.

Using Eqs. (2) and (3) to replace the corresponding entropies in Eq. (1), we have:

$$\begin{aligned} & \left[ \frac{1}{T^{res}} dU^{res} + \frac{P^{res}}{T^{res}} dV^{res} - \sum_j \frac{\mu_j^{res}}{T^{res}} dn_j^{res} \right] + \left[ \frac{1}{T^L} dU^L + \frac{P^L}{T^L} dV^L - \sum_i \frac{\mu_i^L}{T^L} dn_i^L \right] \\ & + \left[ \frac{1}{T^{LM}} dU^{LM} - \frac{\sigma^{LM}}{T^{LM}} dA^{LM} - \sum_i \frac{\mu_i^{LM}}{T^{LM}} dn_i^{LM} \right] \\ & + \left[ \frac{1}{T^M} dU^M + \frac{P^M}{T^M} dV^M - \sum_i \frac{\mu_i^M}{T^M} dn_i^M \right] \\ & + \left[ \frac{1}{T^{MD}} dU^{MD} - \frac{\sigma^{MD}}{T^{MD}} dA^{MD} - \sum_i \frac{\mu_i^{MD}}{T^{MD}} dn_i^{MD} \right] \\ & + \left[ \frac{1}{T^D} dU^D + \frac{P^D}{T^D} dV^D - \sum_i \frac{\mu_i^D}{T^D} dn_i^D \right] = 0 \end{aligned} \quad (4)$$

Next, the constraints of the system must be specified. It is considered that n-heptane is component (1), toluene is (2), water is (3) and n-dodecane is (4). The constraints of the system are the followings:

- (i) There is no mass transfer between the system and the reservoir. For components in the ELM system, n-heptane does not dissolve in water, therefore exist only in the internal droplets and the droplet-membrane interface. Toluene dissolves in water and transfer to the external phase, hence it exists in all of the phases and interfaces. Water does not dissolve in the internal or external phases, and it can only exist in the membrane and the two interfaces. For n-dodecane cannot dissolve in water, it only exists in the external phase and the external-membrane interface. Therefore, the constraints regarding numbers of moles are:

$$dn_j^{res} = 0 \tag{5}$$

$$dn_1^D + dn_1^{MD} = 0 \tag{6}$$

$$dn_2^D + dn_2^{MD} + dn_2^M + dn_2^{LM} + dn_2^L = 0 \tag{7}$$

$$dn_3^M + dn_3^{LM} + dn_3^{MD} = 0 \tag{8}$$

$$dn_4^L + dn_4^{LM} = 0 \tag{9}$$

- (ii) The system together with the reservoir are isolated, and their energy is conserved, therefore we have:

$$dU^{res} + dU^L + dU^{LM} + dU^M + dU^{MD} + dU^D = 0 \tag{10}$$

- (iii) There system exchange volume with the reservoir:

$$dV^{res} + dV^L + dV^M + dV^D = 0 \tag{11}$$

The geometric relations for the volumes and the interfacial areas can all be expressed in terms of the radius of the droplets ( $r_D$ ), the radius of the globule ( $r_M$ ), and the number of droplets ( $N_{drops}$ ):

$$V^D = \left(\frac{4}{3}\pi r_D^3\right) N_{drops} \tag{12}$$

$$V^M = \frac{4}{3}\pi r_M^3 - \left(\frac{4}{3}\pi r_D^3\right) N_{drops} \tag{13}$$

$$A^{MD} = (4\pi r_D^2) N_{drops} \tag{14}$$

$$A^{LM} = 4\pi r_M^2 \tag{15}$$

Then the differentials of the volumes and areas can both be expressed in terms of the differentials of the corresponding radii  $r_D$  and  $r_M$ .

By incorporating the governing constraints of the system (Eqs. (5) to (11)) into Eq. (4), with some algebraic manipulation, Eq. (4) yields to:

$$\begin{aligned} & \left(\frac{1}{T^L} - \frac{1}{T^{res}}\right) dU^L + \left(\frac{1}{T^M} - \frac{1}{T^{res}}\right) dU^M + \left(\frac{1}{T^D} - \frac{1}{T^{res}}\right) dU^D + \left(\frac{1}{T^{LM}} - \frac{1}{T^{res}}\right) dU^{LM} \\ & + \left(\frac{1}{T^{MD}} - \frac{1}{T^{res}}\right) dU^{MD} + \left(\frac{\mu_1^D}{T^D} - \frac{\mu_1^{MD}}{T^{MD}}\right) dn_1^{MD} + \left(\frac{\mu_2^D}{T^D} - \frac{\mu_2^{MD}}{T^{MD}}\right) dn_2^{MD} \\ & + \left(\frac{\mu_2^D}{T^D} - \frac{\mu_2^M}{T^M}\right) dn_2^M + \left(\frac{\mu_2^D}{T^D} - \frac{\mu_2^{LM}}{T^{LM}}\right) dn_2^{LM} + \left(\frac{\mu_2^D}{T^D} - \frac{\mu_2^L}{T^L}\right) dn_2^L \\ & + \left(\frac{\mu_3^M}{T^M} - \frac{\mu_3^{MD}}{T^{MD}}\right) dn_3^{MD} + \left(\frac{\mu_3^M}{T^M} - \frac{\mu_3^{LM}}{T^{LM}}\right) dn_3^{LM} + \left(\frac{\mu_4^L}{T^L} - \frac{\mu_4^{LM}}{T^{LM}}\right) dn_4^{LM} \\ & + \left(\frac{P^L}{T^L} - \frac{P^{res}}{T^{res}}\right) dV^L \\ & + \left[\frac{P^{res}}{T^{res}}(-4\pi r_M^2) + \frac{P^M}{T^M}(4\pi r_M^2) - \frac{\sigma^{LM}}{T^{LM}}(8\pi r_M)\right] dr_M \\ & + \left[\frac{P^M}{T^M}(-4\pi r_D^2(N_{drops})) + \frac{P^D}{T^D}(4\pi r_D^2(N_{drops})) - \frac{\sigma^{LM}}{T^{LM}}(8\pi r_D(N_{drops}))\right] dr_D = 0 \end{aligned} \tag{16}$$

For Eq. (16) to be valid, each coefficient of every independent variation must be zero. This yields to the conditions for equilibrium, including thermal, mechanical and chemical equilibria:

$$T^{res} = T^L = T^{LM} = T^M = T^{MD} = T^D \tag{17}$$

$$P^L = P^{res} \tag{18}$$

$$P^M - P^L = \frac{2\sigma^{LM}}{r_M} \tag{19}$$

$$P^D - P^M = \frac{2\sigma^{MD}}{r_D} \quad (20)$$

$$\mu_1^D = \mu_1^{MD} \quad (21)$$

$$\mu_2^D = \mu_2^L = \mu_2^M = \mu_2^{LM} = \mu_2^{MD} \quad (22)$$

$$\mu_3^M = \mu_3^{LM} = \mu_3^{MD} \quad (23)$$

$$\mu_4^L = \mu_4^{LM} \quad (24)$$

Equations (19) and (20) are called Young–Laplace equation<sup>35</sup>. Due to the curvature of the interfaces, the pressures of the phases at each side of the interface are not the same at the equilibrium condition<sup>35</sup>. This pressure difference is especially considerable between the membrane and internal phases, due to the nanometric curvature of the membrane-internal phase interface.

The equation that expresses the chemical potential of each component  $i$  in a nonideal, incompressible liquid phase is<sup>38</sup>:

$$\mu_i(T, P, x_i) = \mu_i^{ref}(T, P_\infty) + \nu_i(P - P_\infty) + RT \ln(x_i \gamma_i) \quad (25)$$

$R, T$  are the gas constant and temperature, and  $\mu_i, \nu_i, x_i$ , and  $\gamma_i$  are the chemical potential, molar volume, mole fraction and activity coefficient of component  $i$ , respectively. Equation (25) is used to express chemical potential of toluene in internal, membrane and external phases:

$$\mu_2^M(T, P, x_2) = \mu_2^{ref}(T, P_\infty) + \nu_2(P^M - P_\infty) + RT \ln(x_2^M \gamma_2^M) \quad (26)$$

$$\mu_2^D(T, P, x_2) = \mu_2^{ref}(T, P_\infty) + \nu_2(P^D - P_\infty) + RT \ln(x_2^D \gamma_2^D) \quad (27)$$

$$\mu_2^L(T, P, x_2) = \mu_2^{ref}(T, P_\infty) + \nu_2(P^L - P_\infty) + RT \ln(x_2^L \gamma_2^L) \quad (28)$$

It should be noted that the terms for the pressure of external, membrane, and internal phases in Eqs. (26) to (28) are related to each other through the interfacial effects (interfacial tensions and the size of the droplet and membrane globules) as obtained by conditions for equilibrium in Eqs. (19) and (20). When Eqs. (26) to (28) are substituted in equilibrium condition of Eq. (22), and combined with other equilibrium conditions in Eqs. (19) and (20), we have the final equations for calculating the molar fractions of components in each phase at equilibrium:

$$\frac{2\nu_2\sigma^{MD}}{r_D} = RT \ln \frac{x_2^M \gamma_2^M}{x_2^D \gamma_2^D} \quad (29)$$

$$2\nu_2 \left( \frac{\sigma^{LM}}{r_M} + \frac{\sigma^{MD}}{r_D} \right) = RT \ln \frac{x_2^L \gamma_2^L}{x_2^D \gamma_2^D} \quad (30)$$

By using Eq. (29) and (30), the equilibrium mole fraction of toluene in each phase can be determined. The activity coefficients are needed to be calculated if the nonideality of the solution is taken into account. The model used here for the activity coefficients in the liquid phases is NRTL (nonrandom two-liquid) model, which is suitable for a wide range of solutions<sup>39</sup>.

$$\ln \gamma_i = \frac{\sum_{j=1}^n \tau_{ji} x_j G_{ji}}{\sum_{k=1}^n x_k G_{ki}} + \sum_{j=1}^n \frac{x_j G_{ij}}{\sum_{k=1}^n x_k G_{kj}} \left( \tau_{ij} - \frac{\sum_{m=1}^n \tau_{mj} x_m G_{mj}}{\sum_{k=1}^n x_k G_{kj}} \right) \quad (31)$$

$$G_{ij} = \exp(-\tau_{ij} \alpha_{ij}) \quad (32)$$

$$\tau_{ij} = \frac{a_{ij}}{RT} \quad (33)$$

where,  $\gamma_i$  and  $x_i$  are the activity coefficient and the mole fraction of component  $i$ , respectively.  $a_{ij}$  is interaction parameter between  $ij$  (cal/mol),  $T$  stands for temperature (K) and  $\alpha_{ij}$  is the nonrandomness for the  $ij$  pair (where  $\alpha_{ij} = \alpha_{ji}$ ).  $G_{ij}$  is the energy parameter of the  $ij$  interaction. The parameter is related to the nonrandomness of the mixture<sup>39</sup>.

The values of the interaction parameter ( $a_{ij}$ ) and nonrandomness ( $\alpha_{ij}$ ) in the NRTL model fitted to experimental data were obtained from the DWSIM software<sup>40</sup>. With  $a_{ij}$  and  $\alpha_{ij}$  obtained from DWSIM software<sup>40</sup>,  $\tau_{ij}$ 's were calculated from Eq. (33), as reported in Table 2.

Any problem can only be solved when the number of unknowns is equal to the number of independent governing equations, that is when the degree of freedom is zero. Therefore to be able to calculate of the molar fractions after reaching equilibrium and to test the consistency of assumptions, it is necessary to determine the values of radii of the droplets and the globule, and the initial moles of each component. The radii of droplets and

$i$	$j$	$\alpha_{ij}$	$\tau_{ij}$	$\tau_{ji}$
1	2	0.2	-1.487	1.371
3	2	0.2	3.013	-0.935
4	2	0.2	1.861	-2

**Table 2.** The coefficients of the NRTL model for liquid mixture in different phases.  $a_{ij}$  and  $\alpha_{ij}$  were obtained from DWSIM software<sup>40</sup>, and  $\tau_{ij}$ 's were calculated from  $a_{ij}$  for each pair at the temperature of 298.15 K.

Component	N-heptane	Toluene	Water	N-dodecane
Molar volume, $v_i$ [m <sup>3</sup> /mole]	$1.465 \times 10^{-4}$	$1.063 \times 10^{-4}$	$1.8 \times 10^{-5}$	$2.271 \times 10^{-4}$

**Table 3.** Molar volume of each of the components at 298 K.

globules are specified based on the sizes on the images of the emulsion in the experimental study<sup>10</sup>. Moreover, assuming the mentioned values for the volumes of the total emulsion and the external phase in the experimental study<sup>10</sup> (1 ml of emulsion dispersed as globules in 3 ml of the external phase), along with the available data of the molar volume of each component, the number of the internal droplets and globules, as well as the initial moles of the components are determined. The data of the molar volume of each component is reported in Table 3<sup>41</sup>.

The internal phase consists of toluene and normal heptane, and its average molar volume ( $\nu_{avg,drop}$ ), assuming ideal mixing, is given by:

$$\nu_{avg,drop} = x_2^D \nu_2 + x_1^D \nu_1 \quad (34)$$

where  $x_2^D$  and  $x_1^D$  are the mole fractions of toluene and n-heptane in the internal droplet, and  $\nu_i$  is the molar volume of component  $i$ .

For the membrane phase volume,  $V^M$ , the volume of all the internal droplets must be subtracted from the globule volume, according to Eq. (13).

An estimation for the number of droplets ( $N_{drops}$ ) can be obtained based on the images of the samples in the experimental study<sup>10</sup>. The total volume of all internal droplets inside the globule is a fraction of the volume of the globule:

$$N_{drops} \left( \frac{4}{3} \pi r_D^3 \right) = B \left( \frac{4}{3} \pi r_M^3 \right) \quad (35)$$

where  $B$  is the packing fraction of globule by the droplets, and is approximately taken to be 0.83, based on the images of the experimental study<sup>10</sup>. Combining Eqs. (35) and (13), the volume of the aqueous membrane solution can be obtained based on radius of globule and the packing fraction.

From the experimental study<sup>10</sup>, 1 ml of emulsion, which is a collection of globules, is dispersed in 3 ml of the external phase (hence the volume ratio of the external phase to the emulsion phase,  $f$ , is 3). However, our system is defined based on one globule inside the associated external phase. Therefore, the numbers of the globules and the volume of the external phase associated to one globule must be determined, so that reasonable numbers for the initial number of moles can be assigned. Considering 1 ml of emulsion as a collection of globules, the number of globules can be calculated:

$$10^{-6} [m^3] = N_{globules} \left( \frac{4}{3} \pi r_M^3 \right) \quad (36)$$

Once the number of globules ( $N_{globules}$ ) is estimated from Eq. (36), taking into account the distribution of these globules in 3 ml of the external phase, the volume of the external phase per one globule can be calculated with a simple proportion. This volume of the external phase is then used for assigning the initial number of moles of n-dodecane:

$$n_4^{initial} = \frac{V^L}{\nu_4} = \frac{f \left( \frac{4}{3} \pi r_M^3 \right)}{\nu_4} \quad (37)$$

where  $f$  is the volume ratio of the external phase to the emulsion phase, as explained before and is taken to be equal to 3, based on the experimental study<sup>10</sup>.

Also, the initial number of moles of water can be assigned based on the volume of the membrane phase,  $V^M$  (that can be obtained based on radius of globule and the packing fraction by combining Eqs. (35) and (13)), and the packing fraction  $B$  (approximately 0.83 based on the experimental study<sup>10</sup>):

$$n_3^{initial} = \frac{V^M}{\nu_3} = \frac{(1-B) \left( \frac{4}{3} \pi r_M^3 \right)}{\nu_3} \quad (38)$$

Sum of the initial numbers of moles of toluene and n-heptane in the defined system can be assigned based on their amount in the initial droplets:

$$n_1^{initial} + n_2^{initial} = N_{drops} \left( \frac{\frac{4}{3} \pi r_D^3}{\nu_{avg,drop}^{initial}} \right) \quad (39)$$

The initial number of moles of toluene can therefore be calculated from the initial mole fraction of toluene in the droplet phase:

$$n_2^{initial} = x_2^{D,initial} \left[ N_{drops} \left( \frac{\frac{4}{3} \pi r_D^3}{\nu_{avg,drop}^{initial}} \right) \right] \quad (40)$$

It should be noted that as the system does not exchange mass with the surrounding, the total number of moles of each component remains the same during the separation.

The procedure to solve Eqs. (29) and (30) to find the equilibrium mole fractions, considering the nonideality of the liquid in each phase, are the following steps:

Step 1) The initial moles of each component should be calculated from Eqs. (37) to (40).

Step 2) Guess a number for the mole fraction of toluene in the droplet phase ( $x_2^{D,guess}$ ), below the initial mole fraction of toluene (which was 0.521 in our case). Also, as an initial guess, assume the activity coefficients of toluene in the membrane and external phases to be 1.

Step 3) Calculate the activity coefficient of toluene in the internal droplet phase using Eq. (31) using the guess value for the mole fraction of toluene in the droplet phase.

Step 4) Calculate the mole fractions of toluene in the membrane and external phase using Eqs. (29) and (30), respectively.

Step 5) Correct the activity coefficients of toluene in the membrane and external phases using Eq. (31), based on the mole fractions obtained from step 4. This correction procedure should continue until the values of the mole fractions of toluene in the membrane and external phases becomes close enough in the two consecutive repeat.

Step 6) Number of moles of toluene in each phase can be calculated, from the calculated mole fractions in step 5, and the total number of moles in each phase. It should be noted that as the solubility of n-heptane and dodecane is almost zero in the water (membrane), these components remain in the phase they initially existed. Therefore, the final number of moles of the n-heptane in the droplet phase, and dodecane in the external phase, is the same as the initial number of moles of each of these components.

Therefore, number of moles of toluene in each of the phases ( $n_2^D, n_2^M$ , and  $n_2^L$ ) can be calculated from:

$$n_2^D = x_2^D (n_2^D + n_1^{initial}) \quad (41)$$

$$n_2^M = x_2^M (n_2^M + n_3^{initial}) \quad (42)$$

$$n_2^L = x_2^L (n_2^D + n_4^{initial}) \quad (43)$$

Step 7) If the sum of the number of moles of toluene in all the phases is close enough to the initial number of moles of toluene, then the guess in step 2 was a good guess, otherwise the procedure must be repeated from step 2.

With the assigned values for the radii of the droplets and the globule, and the total numbers of moles of the components, and with the governing equations, the equilibrium mole fraction of toluene can be calculated. The percentage of extraction of toluene can then be obtained:

$$\%extraction = \frac{x_2^{D,initial} - x_2^D}{x_2^{D,initial}} \times 100 \quad (44)$$

The flowchart of solving procedure is provided for better understanding these steps in Fig. 4.

If the liquid solution of each phase is assumed to be ideal solution, the steps for calculating and correcting activity coefficients should be ignored as the activity coefficients of each component in each phase is 1.

## Results and discussion

The effects of the size and number of internal droplets, ideal or non-ideal assumption for the liquid solutions, and value of the interfacial tension (changes as the result of surfactant) on the percentage of extraction are investigated. Different scenarios have been investigated at a temperature of 298.15 Kelvin and pressure of 1 atm.

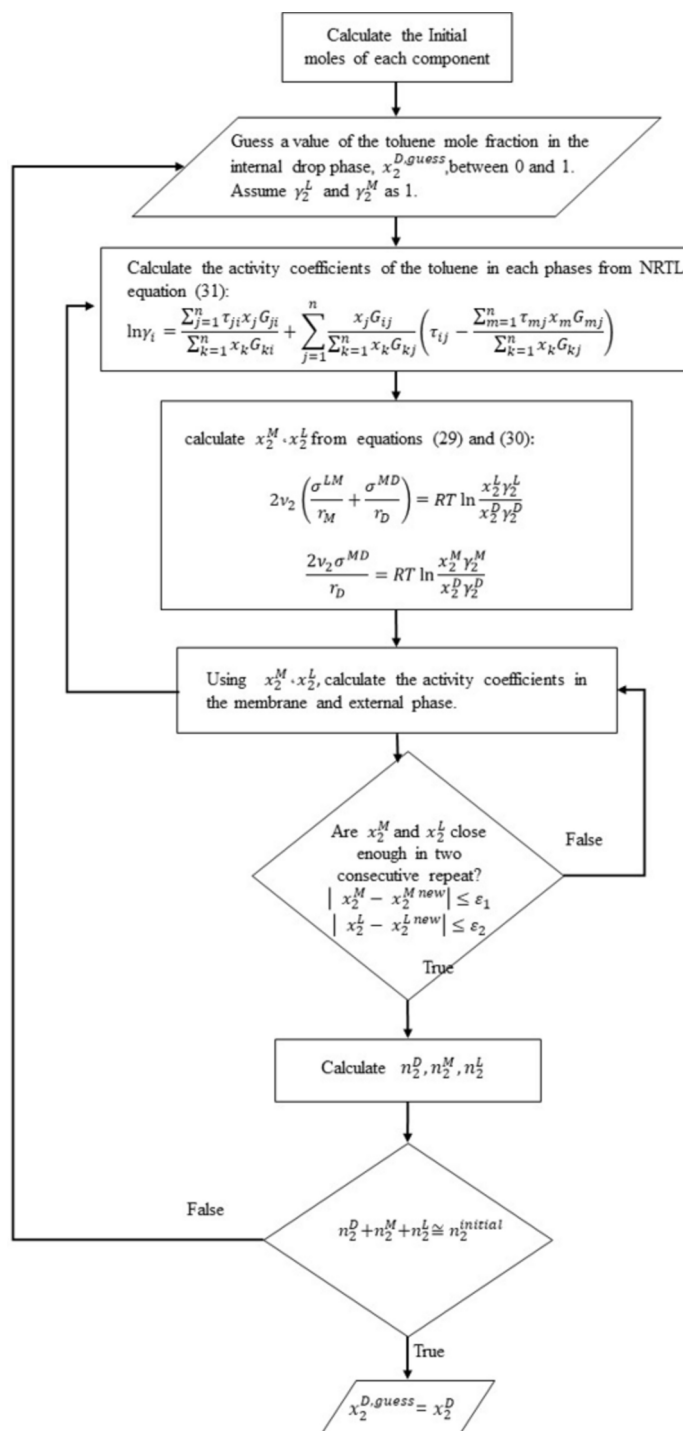


**Fig. 4.** Flowchart of the steps to calculate mole fraction of toluene (target of the separation) in the internal phase for a system representing emulsion liquid membrane with a simple mechanism (no reaction). Initially the internal phase contained toluene and n-heptane, the membrane phase was assumed to be only water, and the external phase was n-dodecane. After separation, only toluene distributes between phases, as only toluene can transfer through the membrane phase.

#### Effect of internal droplet size and assumption of ideal or non-ideal solution

In this section, by specifying the radius of the globule, the initial moles of components in the system (based on the experimental data<sup>10</sup>), and the values of interfacial tensions between the internal-membrane and membrane-external phases constant, the effect of the radius size of the internal droplets, and consequently the number of internal droplets, on the percentage of toluene extraction has been studied in two cases: once assuming ideal mixtures (activity coefficients of 1), and another time under non-ideal conditions, with activity coefficients

calculated from NRTL model (Eq. (31) and the coefficients presented in Table 2). It should be noted that the interfacial tensions are set to a fixed number and the impact of the surfactant on the interfacial tension has not been considered in this section.

The initial number of moles of components have been assigned using Eqs. (37) to (40), according to the experimental conditions mentioned in the reference article<sup>10</sup> and considering the globule radius of 30  $\mu\text{m}$ . Using Eq. (35), the number of droplets can be calculated. The interfacial tension of the membrane-internal interface is assumed to be the average of the interfacial tension between n-heptane and water<sup>42</sup> and toluene and water<sup>43</sup>, and the interfacial tension of the membrane-external interface is assumed to be the interfacial tension of n-dodecane and water<sup>44</sup> in pure conditions, without the effect of any surfactants, at a temperature of 298.15 Kelvin and pressure of 1 atmosphere.

In this section, calculations have been performed for internal droplet radii of 15  $\mu\text{m}$ , and 80, 50, 20, 12, and 6 nm. The initial numbers of moles are  $3.89 \times 10^{-10}$  mol for toluene and  $3.57 \times 10^{-10}$  mol for n-heptane,  $1.07 \times 10^{-9}$  mol for water and for  $1.5 \times 10^{-9}$  mol for n-dodecane. The interfacial tension for membrane-internal interface is 39 mN/m and for membrane-external interface is 53.7 mN/m. As the droplet radius becomes smaller, the number of internal droplets increases, and the number of moles of toluene and n-heptane in each droplet decrease. Figure 5 illustrates the effect of droplet radius, in orders of nm, on the percentage of toluene for two cases of assuming the liquid solutions to be ideal or nonideal.

The results show that as the radius of the internal droplet decreases to the nanoscale, due to the noticeable effect of curvature, the percentage of toluene extraction increases. More toluene is transferred from the internal phase to the external phase. According to previous research<sup>3,5,7,8,12</sup>, smaller particles lead to a larger interfacial area between the membrane and internal phases, enhancing mass transfer, reducing the weight force's impact on droplets' stability, and delaying coalescence<sup>5</sup>. It should be noted that generating smaller particles requires higher agitator rotation speed, which can lead to the emulsion globule's rupture<sup>8</sup>. In most processes, ultrasonic homogenizers are used for producing nanoscale droplets<sup>3</sup>.

Regarding the assumption of ideal or non-ideal behavior of the mixture, assuming ideality means neglecting the difference in the interaction energy of components with each other. In an ideal solution, the interactions between unlike molecules  $ij$  are assumed to be identical to those between like molecules  $ii$  or  $jj$ , which simplifies the modeling and leads to activity coefficients equal to 1. Conversely, in a non-ideal solution, differences in molecular shape, size, and polarity cause the  $ij$  interactions to differ from  $ii$  /  $jj$  interactions. These deviations alter the activity coefficients, chemical potentials, and therefore the component distribution. Non-ideal behavior typically results in lower extraction efficiency compared to ideal solution assumption. In the system investigated in this paper, the activity coefficient of toluene is the smallest in the external phase because of the more attractive interaction between toluene-dodecane. The activity coefficient of toluene gets slightly higher in the droplet solution, and is the largest in the aqueous membrane phase, as toluene-water interaction is the least attractive of all. Therefore, with the real (non-ideal) solution assumption, extraction efficiency decreases compared to assuming ideal solution, due to the limitation of the aqueous phase.

The mole fraction of toluene after extraction in the internal droplet versus size of droplet is presented in Fig. 6.

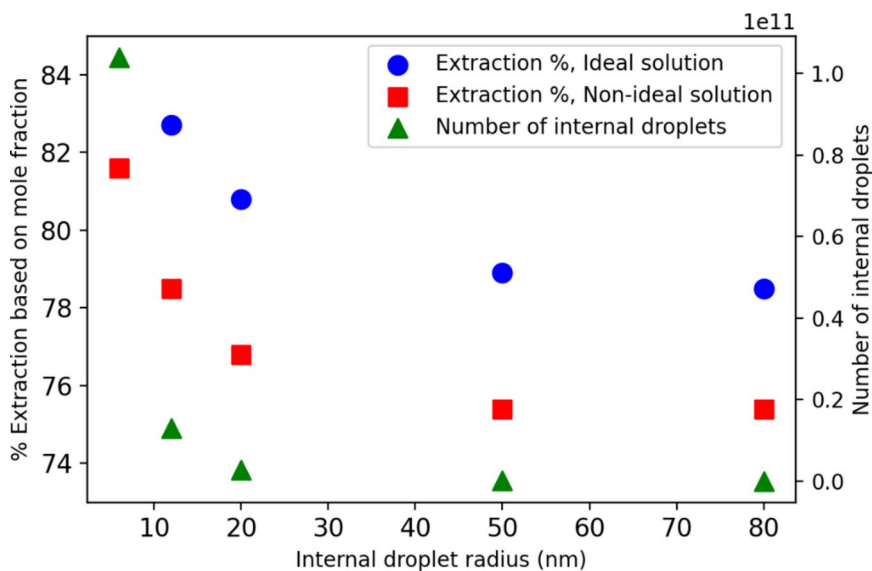


**Fig. 5.** The effect of internal droplet radius in orders of nanometer on the percentage of toluene extraction, for a system with globule radius of 30  $\mu\text{m}$ , considering the liquid solutions to be either ideal or non-ideal mixtures. The initial numbers of moles are  $3.89 \times 10^{-10}$  mol of toluene and  $3.57 \times 10^{-10}$  mol of n-heptane,  $1.07 \times 10^{-9}$  mol of water, and  $1.5 \times 10^{-9}$  mol of n-dodecane. The reservoir temperature and pressures are 298.15 K and 1 atm. The values used for the interfacial tension between the membrane-internal phases is 39 mN/m and for external-membrane phase is 53.7 mN/m.

When the droplet radius gets larger to 15  $\mu\text{m}$ , there is only one internal droplet. This configuration yields the lowest extraction percentage compared to droplets with smaller sizes, and due to the micrometer scale, the interfacial curvature effect is not significant.

In another scenario, investigations were performed for a globule radius of 2000  $\mu\text{m}$  and internal droplet sizes of 300, 150, 30, and 3  $\mu\text{m}$ . The initial numbers of moles are  $1.36 \times 10^{-4}$  mol for toluene and  $1.25 \times 10^{-4}$  mol for n-heptane,  $3.16 \times 10^{-4}$  mol for water and for  $4.43 \times 10^{-4}$  mol for n-dodecane. Results are presented in Fig. 7, with the calculation procedure same as the previous case.

When the droplet radius is in the order of  $\mu\text{m}$ , the effect of size of the droplet (curvature effect between the two phases) is less noticeable. The percentage of toluene extraction varies from 64.45% for the internal droplet radius of 300  $\mu\text{m}$  to 66.6% for the internal droplet radius of 30  $\mu\text{m}$ . It's evident that this change is relatively subtle compared to the nanoscale internal droplet radius. In the nanoscale range, the percentage of toluene extraction changes from 75.4% for the internal droplet radius of 80 nm to 81.6% for the internal droplet radius of 6 nm, and the curvature effect is quite noticeable.

### The effect of the interfacial tension, due to the surfactant

Surfactants are used to enhance emulsion stability by reducing the interfacial tension when their concentration increases<sup>7</sup>. Therefore, type and amount of the surfactant concentration have a significant impact on the extraction percentage, as well as the stability. Surfactants prevent swelling or rupturing of the emulsion<sup>3</sup>. However, high surfactant concentration and excessive stability can hinder the demulsification process in the final stage. Thus an optimal surfactant concentration must be used<sup>3</sup>. In the experimental study<sup>10</sup>, the optimal surfactant concentration chosen for toluene separation from n-heptane is 3% w/v of surfactant/solution. If the concentration is lower than the optimal value, the number of internal droplets become very low, and their sizes get larger, potentially leading to the instability of the globule and separation of internal droplets from the membrane phase. Similarly, if the surfactant concentration exceeds 3%, due to the creaming effect and the increased viscosity of the emulsion, the internal droplets coalesce and become unstable, leading to their dissolution in the external phase<sup>10</sup>.

In this section, the effect of the values of the interfacial tensions of the membrane-internal and membrane-external interfaces on the separation are investigated. The system parameters are similar to those for a system with the globule radius of 30  $\mu\text{m}$  considering non-ideal mixture. The initial number of moles are  $3.89 \times 10^{-10}$  mol for toluene,  $3.57 \times 10^{-10}$  mol for n-heptane,  $1.07 \times 10^{-9}$  mol for water, and  $1.5 \times 10^{-9}$  mol for n-dodecane. The temperature and pressure are 298.15 K and 1 atm. Figure 8 illustrates the effect of surface tensions on the percentage of toluene extraction as a function of the internal droplet radius.

As the interfacial tension decreases with increased amount of surfactant, the nominator ( $2\sigma$ ) in the Young–Laplace relation (Eqs. (19) and (20)) decreases. Therefore, the effect of droplet curvature on the mole fraction and extraction percentage of toluene is reduced, because of the smaller surface tension. For example, assuming the interfacial tension of 3.8 mN/m for the membrane-droplet interface, and 5.4 mN/m for the membrane-external interface, the toluene extraction percentage is 74.5 when the internal droplet radius is 100 nm, and 75.2 when the internal droplet radius is 6 nm. That is only 0.93% increase in the percentage of the toluene extraction, as the internal droplet radius decreases by 94%. The use of surfactant with the appropriate concentration, can

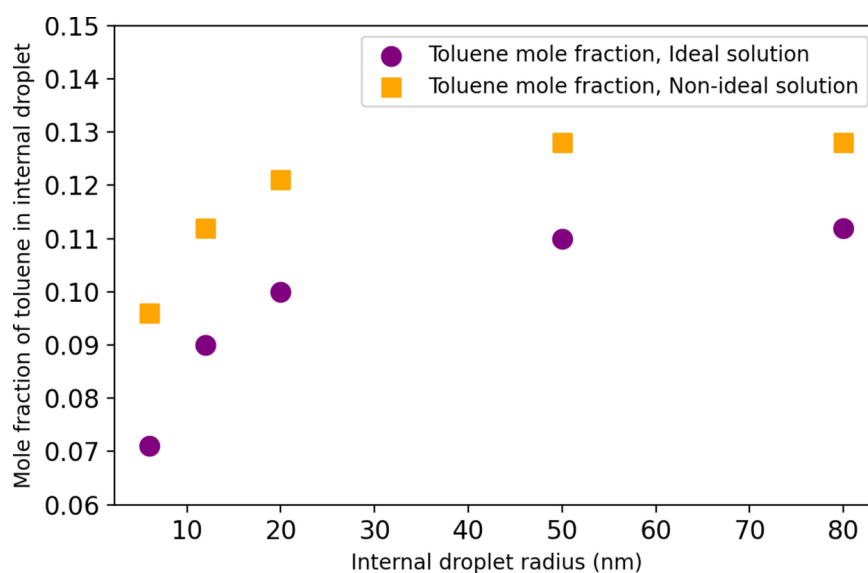


**Fig. 6.** The effect of internal droplet radius in orders of nanometer on the mole fraction of toluene in each internal droplet, for a system with globule radius of 30  $\mu\text{m}$ , considering the liquid solutions to be either ideal or non-ideal mixtures. The initial numbers of moles is  $3.89 \times 10^{-10}$  mol of toluene and  $3.57 \times 10^{-10}$  mol of n-heptane,  $1.07 \times 10^{-9}$  mol of water, and  $1.5 \times 10^{-9}$  mol of n-dodecane. The reservoir temperature and pressures are 298.15 K and 1 atm. The values used for the interfacial tension between the membrane-internal phases is 39 mN/m and for external-membrane phase is 53.7 mN/m.

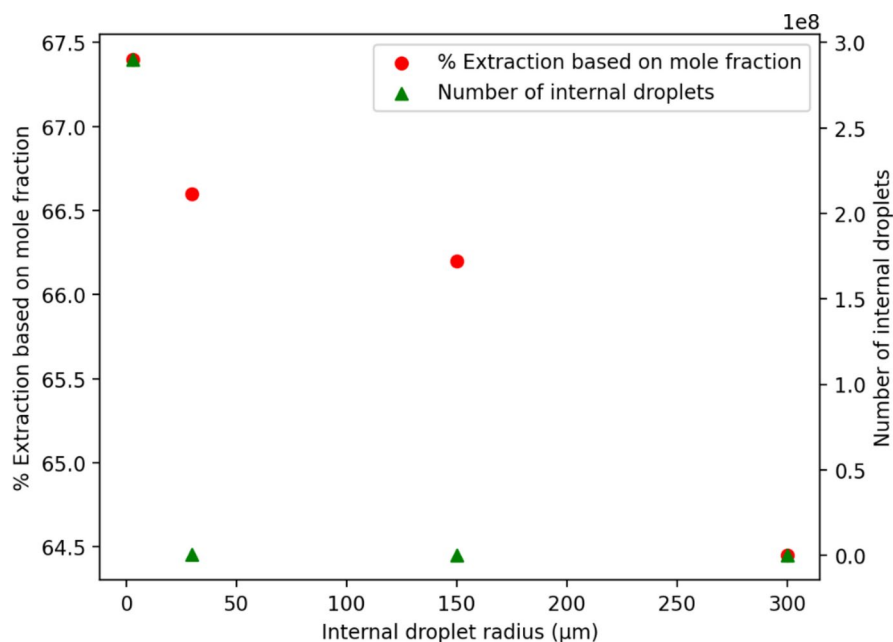


**Fig. 7.** The effect of internal droplet radius, in order of micrometer scale, on the percentage of toluene extraction, for a system with a globule of radius of 2000  $\mu\text{m}$ , considering phases to be non-ideal mixture. The initial number of moles are  $1.36 \times 10^{-4}$  mol of toluene and  $1.25 \times 10^{-4}$  mol n-heptane,  $3.16 \times 10^{-4}$  mol of water and  $4.43 \times 10^{-4}$  mol of n-dodecane. The reservoir temperature and pressures are 298.15 K and 1 atm. The values used for the interfacial tension between the membrane-internal phases is 39 mN/m and for external-membrane phase is 53.7 mN/m.

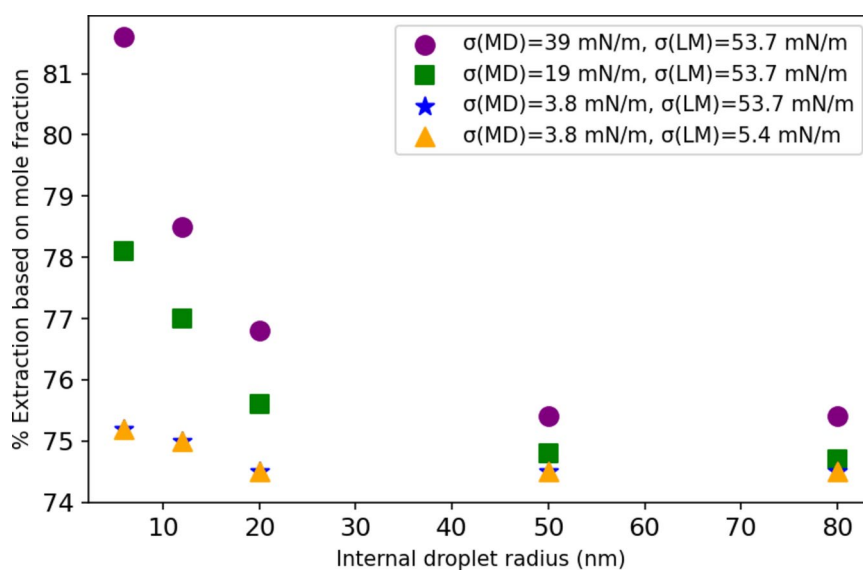


**Fig. 8.** The effect of surface tension on the percentage of extraction of toluene as a function of the internal droplet radius, for separation of toluene from n-heptane, using emulsion liquid membrane with simple mechanism. The system has a globule with the radius of 30  $\mu\text{m}$ , The initial numbers of moles are  $3.89 \times 10^{-10}$  mol for toluene,  $3.57 \times 10^{-10}$  mol for n-heptane,  $1.07 \times 10^{-9}$  mol for water and  $1.5 \times 10^{-9}$  mol for n-dodecane. The reservoir temperature and pressure are 298.15 K and 1 atm.

reduce the need for fine particles and lower the energy consumption in the process as we can reach to a certain amount of extraction even with bigger droplets.

## Conclusions

Emulsion liquid membranes (ELMs) are a type of double emulsion with three phases in the form of internal/membrane/external emulsion, they offer a promising method for separation. The membrane phase allows selective passage of the target substance from the internal phase to the external phase or vice versa. The separation mechanism in emulsion liquid membranes is either a simple (without reaction) or a facilitated mechanism. In this study, we have investigated the effect of parameters such as the interfacial curvature and the droplet size, as well as the value of the interfacial tension, on the separation of toluene from n-heptane, according to a previous experimental study. The results suggest that the smaller nano-sized internal droplets, the better mass transfer, and the higher toluene extraction percentages, due to the increased interfacial area between the membrane and internal phase, and also higher pressure in the inner phase. For the accurate (pseudo-)equilibrium mole fractions of the toluene after the separation, it is important to consider the effect of nanoscale internal droplet size. This nanoscale internal droplet size results in pressure difference between the internal and the membrane phases according to the Young–Laplace equation.

Additionally, the influence of the surfactants on the percentage of extraction was examined. Higher surfactant concentration and reduced interfacial tension can impact extraction percentages due to the reduced droplet size, according to the Young–Laplace equation. On the other hand, because of the smaller interfacial tension, the effects of the interface curvature (even at nanoscale) on the extraction percentage, becomes inconspicuous. This suggests that by employing an adequate quantity of surfactant, and creating low interfacial tension, achieving the desired extraction percentage is feasible even with larger internal droplet sizes. This, in turn, could mitigate the necessity for high rotational speeds and energy consumption.

Furthermore, the project considered the effect of the non-ideal behavior of the solution. The obtained extraction percentages might deviate from reality if ideal assumptions are made, due to not accounting for the differences in interactions between like and unlike components.

The chosen system for this study was ELMs with a simple mechanism without chemical reactions between phases, allowing for some initial mathematical modeling. Considering that the facilitated (with reactions) emulsion liquid membranes are more widely used, the next step involves investigating systems with chemical reactions. The effect of other parameters, such as the type and concentration of inhibiting and carrier agents on the extraction percentage can be investigated, with a similar approach.

## Data availability

All data generated or analysed during this study are included in this published article.

Received: 31 October 2024; Accepted: 17 February 2025

Published online: 21 February 2025

## References

- Li, N. N. Separation of hydrocarbons by liquid membrane permeation. *Ind. Eng. Chem. Process Des. Dev.* **10**(2), 215–221. <https://doi.org/10.1021/i260038a014> (1971).
- Mousumi Chakraborty, Chiranjib Bhattacharya, and S. D. Liquid Membranes: Principles and Applications in Chemical Separations and Wastewater Treatment. In *Liquid Membranes: Principles and Applications in Chemical Separations and Wastewater Treatment* Vol. 9, 445 (Elsevier, 2010). <https://doi.org/10.1016/B978-0-444-53218-3.00001-5>.
- Ahmad, A. L., Kusumastuti, A., Derek, C. J. C. & Ooi, B. S. Emulsion liquid membrane for heavy metal removal: An overview on emulsion stabilization and destabilization. *Chem. Eng. J.* **171**(3), 870–882. <https://doi.org/10.1016/j.cej.2011.05.102> (2011).
- Zereshki, S., Shokri, A. & Karimi, A. Application of a green emulsion liquid membrane for removing copper from contaminated aqueous solution: Extraction, stability, and breakage study using response surface methodology. *J. Mol. Liq.* **325**, 115251. <https://doi.org/10.1016/j.molliq.2020.115251> (2021).
- Zaulkiflee, N. D., Ahmad, A. L., Sugumaran, J. & Lah, N. F. C. Stability study of emulsion liquid membrane via emulsion size and membrane breakage on acetaminophen removal from aqueous solution using TOA. *ACS Omega* **5**(37), 23892–23897. <https://doi.org/10.1021/acsomega.0c03142> (2020).
- Shirasangi, R., Kohli, H. P., Gupta, S. & Chakraborty, M. Separation of methylparaben by emulsion liquid membrane: Optimization, characterization, stability and multiple cycles studies. *Colloids Surf. A Physicochem. Eng. Asp.* **597**(April), 124761. <https://doi.org/10.1016/j.colsurfa.2020.124761> (2020).
- Kumar, A., Thakur, A. & Panesar, P. S. Recent developments on sustainable solvents for emulsion liquid membrane processes. *J. Clean. Prod.* **240**, 118250. <https://doi.org/10.1016/j.jclepro.2019.118250> (2019).
- Abbassian, K. & Kargari, A. Modification of membrane formulation for stabilization of emulsion liquid membrane for extraction of phenol from aqueous solutions. *J. Environ. Chem. Eng.* **4**(4), 3926–3933. <https://doi.org/10.1016/j.jece.2016.08.030> (2016).
- Floarea, O. Emulsion liquid membranes stability. *UPB Sci. Bull. Ser. B Chem. Mater. Sci.* **70**(3), 1454–2331 (2008).
- Chakraborty, M. & Bart, H. J. Emulsion liquid membranes: Role of internal droplet size distribution on toluene/n-heptane separation. *Colloids Surf. A Physicochem. Eng. Asp.* **272**(1–2), 15–21. <https://doi.org/10.1016/j.colsurfa.2005.07.002> (2006).
- Laki, S. & Kargari, A. Extraction of silver ions from aqueous solutions by emulsion liquid membrane. *J. Membr. Sci. Res.* **2**(1), 33–40. <https://doi.org/10.22079/JMSR.2016.15876> (2016).
- Kargari, A., Kaghazchi, T., & Sohrabi, M. Application of experimental design to emulsion liquid membrane pertraction of gold(III) ions from aqueous solutions. *Iran. J. Chem. Eng.* **3** (1) (2006).
- Othman, N. et al. Easy removing of phenol from wastewater using vegetable oil-based organic solvent in emulsion liquid membrane process. *Chin. J. Chem. Eng.* **25**(1), 45–52. <https://doi.org/10.1016/j.cjche.2016.06.002> (2017).
- Mohammadi, S. et al. Phenol removal from industrial wastewaters: A short review. *Desalin. Water Treat.* **53**(8), 2215–2234. <https://doi.org/10.1080/19443994.2014.883327> (2015).
- Hussein, M. A., Mohammed, A. A. & Atiya, M. A. Application of emulsion and Pickering emulsion liquid membrane technique for wastewater treatment: An overview. *Env. Sci. Pollut. Res.* **26**, 36184–36204. <https://doi.org/10.1007/s11356-019-06652-3> (2019).
- Kumar, A., Thakur, A. & Panesar, P. S. A review on emulsion liquid membrane (ELM) for the treatment of various industrial effluent streams. *Rev. Environ. Sci. Biotechnol.* **18**(1), 153–182. <https://doi.org/10.1007/s11157-019-09492-2> (2019).
- Mohd Najib, S. B. & Kamaruddin, K. S. N. Removal of carbon dioxide by emulsion liquid membrane containing blended amine. *Adv. Mater. Res.* **1113**, 481–485. <https://doi.org/10.4028/www.scientific.net/amr.1113.481> (2015).

18. Rosly, M. B. et al. Effect and optimization parameters of phenol removal in emulsion liquid membrane process via fractional-factorial design. *Chem. Eng. Res. Des.* **145**, 268–278. <https://doi.org/10.1016/j.cherd.2019.03.007> (2019).
19. Chakraborty, M. & Bart, H. J. Separation of toluene and N-heptane through emulsion liquid membranes containing Ag<sup>+</sup> as carrier. *Chem. Eng. Technol.* **28**(12), 1518–1524. <https://doi.org/10.1002/ceat.200500239> (2005).
20. Kaghazchi, T., Kargari, A., Yegani, R. & Zare, A. Emulsion liquid membrane pertraction of L-lysine from dilute aqueous solutions by D2EHPA mobile carrier. *Desalination* **190**(1–3), 161–171. <https://doi.org/10.1016/j.desal.2005.06.031> (2006).
21. Fathi, S. A. M., Yafian, M. R. & Kargari, A. Water-in-oil emulsion liquid membrane transport of L-cysteine. *Sep. Sci. Technol.* **48**(1), 105–112. <https://doi.org/10.1080/01496395.2012.675001> (2013).
22. Thien, M. P., & Hattton, T. A. *Liquid Emulsion Membranes and Their Applications in Biochemical Processing*, Vol. 23. <https://doi.org/10.1080/01496398808063141> (1988).
23. Fathi, S. A. M., Yafian, M. R., Kargari, A. & Matt, D. Emulsion liquid membrane pertraction of L-cysteine from sodium chloride aqueous solutions mediated by a narrow rim phosphorylated cone-shaped calix[4]arene. *J. Iran. Chem. Soc.* **9**(5), 783–789. <https://doi.org/10.1007/s13738-012-0079-2> (2012).
24. Lende, A. B. et al. Emulsion ionic liquid membranes (EILMs) for removal of Pb(II) from aqueous solutions. *RSC Adv.* **4**(94), 52316–52323. <https://doi.org/10.1039/c4ra06485b> (2014).
25. Prajapati, S., Dohare, R. K., Srivastava, A., Imdad, S. & Agarwal, M. Preparation of an emulsion membrane utilizing ionic liquids for the efficient removal of cationic dye: Extraction and breakage study. *Monatshfte fur Chemie* **155**(12), 1209–1223. <https://doi.org/10.1007/s00706-024-03265-6> (2024).
26. Khan, H. W., Elgharrawy, A. A. M., Bustam, M. A., Goto, M. & Moniruzzaman, M. Vegetable oil-ionic liquid-based emulsion liquid membrane for the removal of lactic acid from aqueous streams: Emulsion size, membrane breakage, and stability study. *ACS Omega* **7**(36), 32176–32183. <https://doi.org/10.1021/acsomega.2c03425> (2022).
27. Tu, F., Park, B. J. & Lee, D. Thermodynamically stable emulsions using Janus dumbbells as colloid surfactants. *Langmuir* **29**(41), 12679–12687. <https://doi.org/10.1021/la402897d> (2013).
28. Sujatha, S., Rajamohan, N., Vasseghian, Y. & Rajasimman, M. Conversion of waste cooking oil into value-added emulsion liquid membrane for enhanced extraction of lead: Performance evaluation and optimization. *Chemosphere* **284**(June), 131385. <https://doi.org/10.1016/j.chemosphere.2021.131385> (2021).
29. Sujatha, S. & Rajasimman, M. Development of a green emulsion liquid membrane using waste cooking oil as diluent for the extraction of arsenic from aqueous solution—Screening, optimization, kinetics and thermodynamics studies. *J. Water Process Eng.* **41**(April), 102055. <https://doi.org/10.1016/j.jwpe.2021.102055> (2021).
30. Ward, C. A. & Levart, E. Conditions for stability of bubble nuclei in solid surfaces contacting a liquid-gas solution. *J. Appl. Phys.* **56**(2), 491–500. <https://doi.org/10.1063/1.333937> (1984).
31. Zargarzadeh, L. & Elliott, J. A. W. Bubble formation in a finite cone: More pieces to the puzzle. *Langmuir* **35**(40), 13216–13232. <https://doi.org/10.1021/acs.langmuir.9b01602> (2019).
32. Hefter G. T. Quantitative solubility studies of the toluene–Water system. *Nist, Iupac SDS-37* (1), 369 (1986).
33. Fischer, K. Components: (1). *Nist, Iupac* **26** (1), 376–384 (1986).
34. Winkelman, J. G. M., Kraai, G. N. & Heeres, H. J. Binary, ternary and quaternary liquid-liquid equilibria in 1-butanol, oleic acid, water and n-heptane mixtures. *Fluid Phase Equilib.* **284**(2), 71–79. <https://doi.org/10.1016/j.fluid.2009.06.013> (2009).
35. Elliott, J. A. W. Gibbsian surface thermodynamics. *J. Phys. Chem. B* **124**(48), 10859–10878. <https://doi.org/10.1021/acs.jpcc.0c05946> (2020).
36. Ulbricht, H., Schmelzer, J., & Mahnke, R. *Thermodynamics of Finite Systems and the Kinetics of First-Order Phase Transitions*. <https://doi.org/10.1007/978-3-322-96427-4> (1988).
37. Schmelzer, J. W. P. & Abyzov, A. S. Thermodynamic analysis of nucleation in confined space: Generalized Gibbs approach. *J. Chem. Phys.* <https://doi.org/10.1063/1.3548870> (2011).
38. Shardt, N. & Elliott, J. A. W. Isobaric vapor – liquid phase diagrams for multicomponent systems with nanoscale radii of curvature. *J. Phys. Chem. B* **122**(8), 2434–2447. <https://doi.org/10.1021/acs.jpcc.8b00167> (2018).
39. Medeiros, D. DWSIM-Process Simulation, Modeling and Optimization Technical Manual. *Gen. Public Licens.* **2016**, No. August.
40. Daniel Medeiros. DWSIM. 2022. <https://dwsim.org/>.
41. Haynes, W. M. *Handbook of Chemistry and Physics* 95th edn. (CRC Press, 2014).
42. Ataev, G. M. Dependence of interfacial tension on the temperature and concentration of stearic acid in a water–n-heptane system. *Russ. J. Phys. Chem. A* **92**(8), 1638–1640. <https://doi.org/10.1134/S0036024418080058> (2018).
43. Toor, A., Helms, B. A. & Russell, T. P. Effect of nanoparticle surfactants on the breakup of free-falling water jets during continuous processing of reconfigurable structured liquid droplets. *Nano Lett.* **17**(5), 3119–3125. <https://doi.org/10.1021/acs.nanolett.7b00556> (2017).
44. Binyaminov, H., Abdullah, F., Zargarzadeh, L. & Elliott, J. A. W. Thermodynamic investigation of Droplet–Droplet and Bubble–Droplet equilibrium in an immiscible medium. *J. Phys. Chem. B* **125**(30), 8636–8651. <https://doi.org/10.1021/acs.jpcc.1c02877> (2021).

## Author contributions

Sh.S. completed the computations and wrote the first draft of the manuscript under the supervision of L.Z. All authors reviewed the manuscript.

## Declarations

## Competing interests

The authors declare no competing interests.

## Additional information

**Supplementary Information** The online version contains supplementary material available at <https://doi.org/10.1038/s41598-025-90774-x>.

**Correspondence** and requests for materials should be addressed to L.Z.

**Reprints and permissions information** is available at [www.nature.com/reprints](http://www.nature.com/reprints).

**Publisher's note** Springer Nature remains neutral with regard to jurisdictional claims in published maps and institutional affiliations.

**Open Access** This article is licensed under a Creative Commons Attribution-NonCommercial-NoDerivatives 4.0 International License, which permits any non-commercial use, sharing, distribution and reproduction in any medium or format, as long as you give appropriate credit to the original author(s) and the source, provide a link to the Creative Commons licence, and indicate if you modified the licensed material. You do not have permission under this licence to share adapted material derived from this article or parts of it. The images or other third party material in this article are included in the article's Creative Commons licence, unless indicated otherwise in a credit line to the material. If material is not included in the article's Creative Commons licence and your intended use is not permitted by statutory regulation or exceeds the permitted use, you will need to obtain permission directly from the copyright holder. To view a copy of this licence, visit <http://creativecommons.org/licenses/by-nc-nd/4.0/>.

© The Author(s) 2025